Research Article

Journal of MASS SPECTROMETRY

Received: 17 July 2009 Accepted: 16 October 2009 Published online in Wiley Interscience: 12 November 2009

(www.interscience.com) DOI 10.1002/jms.1695

Characterization of major degradation products of an adenosine A_{2A} receptor antagonist under stressed conditions by LC-MS and FT tandem MS analysis

Li-Kang Zhang* and Birendra N. Pramanik

Parkinson's disease (PD) is a very serious neurological disorder, and current methods of treatment fail to achieve long-term control. SCH 420814 is a potent, selective and orally active adenosine A_{2A} receptor antagonist discovered by Schering-Plough. Stability testing provides evidence of the quality of a bulk drug when exposed to the influence of environmental factors. Understanding the drug degradation profiles is critical to the safety and potency assessment of the drug candidate for clinical trials. As a result, identification of degradation products has taken an important role in drug development process. In this study, a rapid and sensitive method was developed for the structural determination of the degradation products of SCH 420814 formed under different forced conditions. The study utilizes a combination of liquid chromatography–tandem-mass spectrometry (LC-MS/MS) and Fourier Transform (FT) MS techniques to obtain complementary information for structure elucidation of the unknowns. This combination approach has significant impact on degradation product identification. A total of ten degradation products of SCH 420814 were characterized using the developed method.

Keywords: antagonist; degradation; FT MS; MS/MS; structure; LC/MS/MS

Introduction

SCH 420814 (2-(furan-2-yl)-7-(2-(4-(4-(2-methoxyethoxy)phenyl) piperazin-1-yl)ethyl)-7H-pyrazolo[4,3-e][1,2,4]triazolo[1,5-c] pyrimidin-5-amine) is a novel chemical entity which is being investigated for the treatment of Parkinson's disease (PD), a very serious neurological disorder.[1–3] The effects of adenosine are mediated through at least four specific cell membrane receptors classified as A_1, A_{2A}, A_{2B} and A_3. These receptors belong to the G protein-coupled receptor class. It is reported that the A_{2A} and A_{2B} receptors can couple to $G_{s/olf}$ proteins that activate adenylate cyclase and increase intracellular levels of cAMP. On the other hand, the A_1 and A_3 receptors decrease cellular cAMP levels through their coupling to G_i proteins, which inhibit adenylate cyclase.[4] Adenosine A_{2A} receptors modulate the release of GABA in the striatum, which appears to regulate the activity of medium spiny neurons. By reducing GABA output, A_{2A} antagonism helps restore normal function in the basal ganglia following dopamine depletion.[5] Thus, A_{2A} antagonism affords a possible treatment for PD.[6–8] SCH 420814 is a potent, selective and orally active adenosine A_{2A} receptor antagonist discovered by Schering-Plough. It exhibits high affinity for both human and rat A_{2A} receptors, with K_i values of 1.1 and 2.5 n*M*, respectively.[1] Moreover, SCH 420814 is more than 1000-fold selective for human A_{2A} receptors over A_1, A_{2B} and A_3 receptors, with K_i values at human A_1, A_{2B} and A_3 receptors of >1000, >1700 and >1000 n*M*, respectively.[1] The compound is currently in the phase II clinical trials.

Stress testing of a drug candidate is a critical component of both drug discovery and drug development.[9] The identification of drug degradation products in various dosage/formulations plays an important role in the drug discovery process. Information on the structures of degradation products can help chemists modify their novel compounds to prepare drug candidates with improved stability. It has been well documented that drug products will undergo physicochemical degradation during manufacturing processes and storage.[10] Understanding the drug degradation profiles is also critical to the safety and potency assessment of the drug candidate for clinical trials. In addition, stress testing can help in the selection of more-stable drug substance salt forms and drug formulations.[11] It is well accepted that the drug degradation in formulations is highly complex and often unpredictable process. The degradation products usually arise from the ingredients used in dosage formulation and/or in the process of formulation where temperature, humidity and light may all play a part. The degradation products are able to be generated from hydrolysis, oxidation, adduct formation, dimerization, rearrangement and often the combination of these processes. To accelerate drug development, various stress-testing protocols had been designed to emulate stresses the compound may experience during manufacturing and storage conditions.[9] These methods expose drug candidates to forced degradation conditions such as acid, base, heat, oxidation and exposure to light.

LC/MS has become the technique of choice in the degradation product studies due to its inherently high level of sensitivity and specificity. There have been a number of reports in the

* *Correspondence to: Li-Kang Zhang, Chemical Research, Schering-Plough Research Institute, 2015 Galloping Hill Road, K-15-1/1945, Kenilworth, NJ 07033, USA. E-mail: li-kang.zhang@spcorp.com*

Chemical Research, Schering-Plough Research Institute, 2015 Galloping Hill Road, Kenilworth, NJ 07033, USA

Journal of MASS SPECTROMETRY

literature that applied LC-MS and LC-MS/MS for characterization of degradation products.[12–28] A procedure for the rapid structure elucidation of drug degradation products induced by acid, base and heat was reported by Rourick *et al*. in 1996.[17] The same group demonstrated that the similar strategy could be applied to obtain the structural information of the degradation products of paclitaxel (Taxol).[19] In 2000, Wu[21] reviewed the application of LC-MS in the analysis of drug degradation products in pharmaceutical formulations under various stress conditions (oxidation, hydrolysis, dimerization and adduct formation with excipients). Feng *et al*.[14] investigated the oxidative degradation products of an antifungal agent, SCH 56 592, by both LC/MS and LC/NMR analysis. Four major oxidative degradation products of SCH 56 592 were characterized, and the oxidations were found to be occurred at the piperazine ring in the center of the drug molecule. More recently, Li *et al*.[29] reported the use of multiple-stage tandem MS (LC-MS^n) technique, in conjunction with mechanism-based stress studies, to identify the drug degradation products in pharmaceutical development.

Exact mass measurements and elemental-composition assignment are essential for the characterization of small molecules.[22] Accurate mass measurement of the product ions, formed in an MS/MS experiment, facilitates the structure elucidation of new or unknown materials.[22] Hybrid quadrupole/time-of-flight MS had been employed for accurate mass measurement for well over a decade.[30–32] The mass measurement precision/accuracy can be ±5 ppm with internal calibration methods. One limitation of the instruments of this type was the narrow ion abundance range over which accurate mass measurements could be made with a high degree of certainty.[30–33] Currently, FT-ICR MS provides the highest mass resolving power and mass accuracy among all the mass spectrometric methods.[22] Using external calibration, FT-ICR MS is capable of achieving mass measurement accuracies of 1 ppm or better.[22] Smith and co-workers recently reported that by using a new trapped-ion cell with improved DC potential harmonicity, they achieved under 0.05 ppm root-mean-square precision.[34] This is impressive application that is not possible with any other known mass spectrometric equipment. Although FT MS has rapidly developed as one of the most effective techniques for the determination of unknowns, its application to drug degradation products characterization is much less routine than for the drug metabolites screening and drug impurities identification.[29,33,35–40] Bai *et al*.[41] evaluated the application of MALDI-FT-ICR MS for the identification of the degradation products of surfactant proteins. They reported that owing to the high-resolving power, FT-ICR MS was found to provide substantial advantages for the structural identification of surfactant proteins and their degradants from complex biological matrixes with high mass accuracy.[41]

The aims of this research were to perform stress studies on SCH 420814 in order to evaluate its inherent stability, and to develop rapid online LC-MS(/MS) and ultra-high resolution FT MS methods to characterize the degradation products. Although the main focus of the study was chemical degradation of SCH 420814 in solutions, the assessment of the physical stability of the stressed tablets by RH4 condition (open dish, 40 °C/75% relative humidity, 1 month) was also exhibited. The research reported here utilized a combination of LC-MS(/MS) and FT MS techniques to obtain complementary information for structural elucidation of the unknowns. Although the LC-MS offered the molecular weight of the degradation product, the LC-MS/MS provided the detailed structural elucidation information. We will also demonstrated that the ultra-high resolving power of the FT MS was a useful tool to measure the accurate mass and to establish the formula of SCH 420814 degradation products for structural assignments.

Experimental

Materials

SCH 420814, 2-(furan-2-yl)-7-(2-(4-(4-(2-methoxyethoxy)phenyl) piperazin-1-yl)ethyl)-7H-pyrazolo[4,3-e][1,2,4]triazolo[1,5-c] pyrimidin-5-amine, was provided by the Chemical Development Group at Schering-Plough Research Institute. The stock solution of SCH 420814 was prepared by dissolving the compound in acetonitrile/water (80 : 20, v : v) at the concentration of 1.0 mg/ml. Triflouroacetic acid (99%) was purchased from Sigma-Aldrich Chemical Co. (St Louis, MO, USA) and used without further purification. Acetonitrile, deionized water and tetrahydrofuran were also obtained from Aldrich Chemical Co. Hydro chloric acid (2N), sodium hydroxide and hydrogen peroxide were obtained from Fisher Scientific (Fair Lawn, NJ, USA).

Sample preparation

For all of the solution stability studies, the stability samples were prepared by mixing a stock solution of SCH 420814 (1 mg/ml) with various media (30 : 70; v : v). Acid and alkaline stress studies were performed in 0.1 N HCl and 0.1 N NaOH at room temperature for 5 days, respectively. The study in oxidation condition was carried out in 1% H_2O_2 for 24 h. The photo stability study was carried out in a quartz cylindrical cell with Teflon stopper (6445A Photostability Chambers, CARON, Marietta, OH, USA). The SCH 420814 solution (acetonitrile/H_2O; 50/50; v/v) was exposed to UV/VIS in a temperature-controlled (25 °C) light chamber. The total UVA and CWF exposure were equal to 208 W h/m^2 and 1.3 million lux-h, respectively. To assess the physical stability of the compound, SCH 420814 was combined with a common tablet excipient. The active/excipient capsule was stored on an open dish (RH4) for 1 month (Lab-Line and Barnstead/Thermolyne EC14075 small stability chamber, Thermo Scientific, Waltham, MA, USA). The HPLC sample solution was prepared by diluting the active/excipient mixture with water/acetonitrile (50 : 50, v : v). Following forced decomposition, all samples are stored at −20 °C to minimize further degradation and allow for future use.

LC-MS, LC-MS/MS, FT MS and LC-FT MS analyses

LC/ESI-MS and LC/ESI-MS/MS analyses were performed on a PE-Sciex QStar Pulsar Q-TOF mass spectrometer (Applied Biosystems, Foster City, CA, USA) coupled to a Shimazu HPLC system, operated in the positive-ion mode. The HPLC system consisted of solvent delivery module (LC-10AT_{VP}), auto injector (SIL-10A_{VP}) and UV-visible dual-wavelength detector (SPD-10A_{VP}) (Shimadzu Corporation, Tokyo, Japan). All HPLC separations were performed at ambient temperature. The samples were analyzed on a reverse-phase C_{18} column (YMC ODS-A, 250 mm × 4.6 mm, I.D., 5 µm) using A (water/tetrahydrofuran/trifluoroacetic acid; 90 : 10 : 0.1, v : v : v) and B (acetonitrile/water/tetrahydrofuran/trifluoroacetic acid; 50 : 40 : 10 : 0.1, v : v : v : v) as mobile phases at a flow rate of 1.0 ml/min. The injection volume was 30 µl and UV detection was set at 262 nm. The mobile phase gradient started at 0% B, and linearly increased to 100% B over 40 min. The tandem MS analysis of all the compounds was performed on the same Q-TOF MS instrument in the MS-MS mode, with Turbo-Ion-Spray ionization.

The collision energy was 35 eV for all the analytes and standards. The time-of-flight was operated with a pulsing frequency of 10 kHz. Calibration was achieved using CsI at *m/z* 133, Verapamil at *m/z* 455 and a peptide (ALILTLVS) at *m/z* 829. The resolution of the time-of-flight was 10 000, full width half maximum (FWHM) at *m/z* 455. The quadrupole mass analyzer was set to unit resolution.

High-resolution MS spectrum were acquired on a Bruker Daltonics APEX IV 70e FT mass spectrometer (Bruker Daltonic, Billerica, MA, USA) equipped an Apollo electrospray ionization source. A source temperature of 120 °C was used for all experiments. The samples were infused at a flow rate of 1 µl/min into the electrospray source, to which a voltage of 3.8 kV was applied. Ions were stored in the source region in a hexapole guide for 2 s and pulsed into the detection cell through a series of electrostatic lenses. Ions were finally trapped in the cell using either gas-assisted dynamic trapping (Xe pulses, upper pressure around 10^{-7} mbar) with front and back trapping voltages of 3.0 and 3.5 V for trapping, reduced to 0.5 and 0.6 V for detection or static trapping. Mass spectra were acquired from *m/z* 120 to 2000 with 1024 K data points, and peaks were automatically labeled using the XMASS 7.08 software (Bruker Daltonik GmbH, Bremen, Germany). The external calibration was achieved using Verapamil at *m/z* 455.2904, a peptide (ALILTLVS) at *m/z* 829.5393 as well as the product ion of ALILTLVS at *m/z* 724.4967 (ALILTLV), 625.4283 (ALILTL) and 512.3443 (ALILT). The resolution of the time-of-flight was 150 000, FWHM at *m/z* 455.2904. For sustained off resonance irradiation collision-induced dissociation (SORI-CID) experiment, the ion to fragment was isolated by radio frequency (rf) ejection of all unwanted ions using both low-voltage single rf pulses at their resonance frequencies and a chirp excitation covering the region of interest. The fragmentation was performed using excitation duration of 400 µs at a frequency 500 Hz higher than the cyclotron frequency of the ion of interest. Xenon was used as the collision gas and introduced several times through a pulsed valve to get a pressure in the cell up to 10^{-7} mbar. The excitation/detection of all fragment ions was performed after a 3 s pumping delay.

LC/ESI-FT MS was performed on the same instrument coupled to an Agilent 1100 series liquid chromatograph (Agilent G1312A binary pump, G1313A Auto sample injector, G1316A Column oven and G1314A VWD UV detector; Agilent Technologies, Wilmington, DE, USA). The base-stressed SCH 420814 was analyzed by LC-FT MS. All HPLC separations were performed at 25 °C. The samples were analyzed on a reverse-phase C_{18} column (YMC ODS-A, 250 mm × 4.6 mm, I.D., 5 µm) using 0.1% formic acid and acetonitrile as a mobile phase at a flow rate over the column of 500 µl/min in the split-flow LC systems. The LC systems were controlled through HyStar version 3.3 (Bruker), and the FT MS was controlled by apexControl 2.0. The injection volume was 10 µl. The mobile phase gradient started at 40% acetonitrile in 0.1% formic acid, and linearly increased to 80% acetonitrile over 6 min, and then linearly increased to 90% in 4 min. The FT MS conditions were the same as those described above for the standards. DataAnalysis 3.3 (Bruker) was applied to process the FT MS data.

Results and Discussion

SCH 420814 structure characterization by LC-MS, LC-MS/MS, and FT MS analyses

To assess the purity of SCH 420814, a MS-friendly HPLC method was developed as described in the experimental section. The synthetic compound was analyzed by both LC/ESI-MS and LC/ESI-MS/MS in positive mode. The ESI source parameters were optimized to reduce the background signals and to minimize fragmentation reactions. The molecular weight of SCH 420814 (Rt 18.5 min) was confirmed to be 503 Da by LC/MS analysis (spectrum not presented). The elemental composition of SCH 420814 was established by high-resolution FT MS (MH^+: $C_{25}H_{30}N_9O_3$). The calculated exact mass and measured mass was 504.2472 and 504.2474 amu, respectively. The mass measurement error of −0.5 ppm was achieved using external calibration. According to the LC-UV and LC-MS data, there was no impurity detected in this batch of SCH 420814.

An initial step in elucidating degradant structures of SCH 420814 is to understand the fragmentation pattern of the drug substance. Extensive tandem-mass spectrometry analysis of the fragmentation pattern of SCH 420814 provides a basis for assessing structural assignment for the degradation products. The ability of FT MS to provide an exact mass measurement for each of the ions produced in tandem MS assists greatly in the investigation of the fragmentation mechanism of SCH 420814. Accurate mass characterization of SCH 420814 (*m/z* 504) was performed on a Bruker FT MS instrument using SORI-CID. Collision-induced decomposition (CID) of the ESI-produced MH^+ precursor generates ions at *m/z* 311, 263, 234 and 206 (Fig. 1). The most abundant product ion (*m/z* 263.1754) observed in the spectrum is formed by a neutral loss of 2-(furan-2-yl)-7H-pyrazolo[4,3-e][1,2,4]triazolo[1,5-c]pyrimidin-5-amine (Fig. 1). It could further decompose to an ion of *m/z* 234.1364 by a loss of ethyl radical in the gas phase (Fig. 1). Two complementary fragment ions of SCH 420814 are also observed at *m/z* 206.1175 and 311.1363 (Fig. 1). The mass measurement errors of these fragment ions are determined to be −0.02, 0.22, 0.51 and 0.53 ppm, respectively (Fig. 1). SCH 420814 was also submitted to LC/MS/MS analysis on a hybrid Qq-TOF instrument. The product-ion spectrum generated from the Q-TOF instrument is dominated by the same fragments as in the FT SORI-CID spectrum (*m/z* 311, 268, 263, 234 and 206) (product-ion spectrum not shown). The relative intensities of these ions recorded on the two instruments are also very similar.

Degradation behaviors of SCH 420814

The forced degradation samples of SCH 420814 (acidic, basic, oxidative and photolytic) were analyzed by LC-MS(/MS) to identify the degradation products. The LC-MS total ion chromatograms (TIC) were obtained for SCH 420814 at each stress conditions (Fig. 2). A total of ten degradation products of SCH 420814 were characterized using extensive tandem MS analysis.

Studies under acidic conditions

After 5 days exposure to the acidic media at room temperature, less than 10% degradation was observed according to the LC/UV data. Three degradation products (**A, B** and **C**) were detected in the acid-stressed sample (Fig. 2(A)), and the relative retention times (RRT) of the three components were found to be 0.61, 0.81 and 0.87, respectively (Fig. 2(A)). According to the LC/MS data, the molecular weight of **A, B** and **C** were determined to be 353, 489 and 477 Da, respectively.

Mass accuracy is critical in establishing compound identity. Accurate mass measurements (i.e. those less than 2 ppm) can aid in the characterization of the degradation products by placing constraints on elemental formulas of the unknowns. In order to obtain the accurate masses of the three components, the acid-stressed SCH 420814 sample was submitted to high-resolution

Journal of MASS SPECTROMETRY

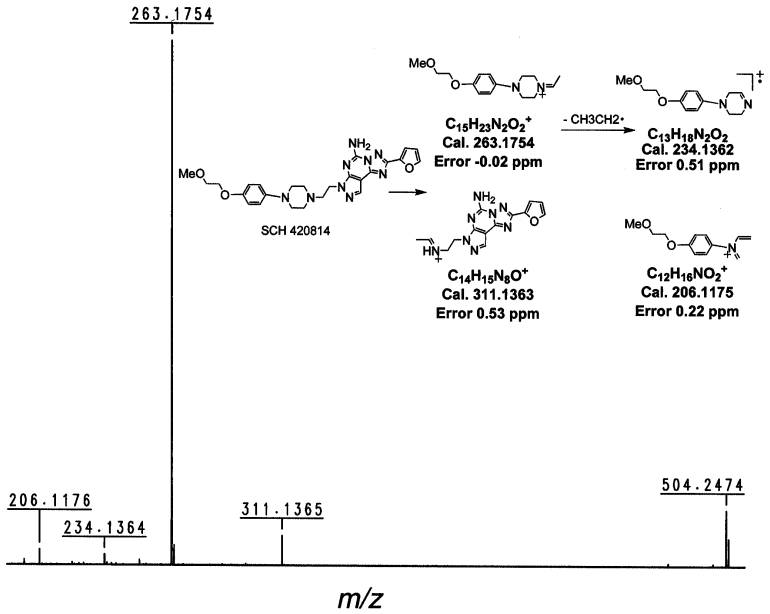

Figure 1. Proposed fragmentation pathways and ESI-FT MS product-ion spectrum of SCH 420814.

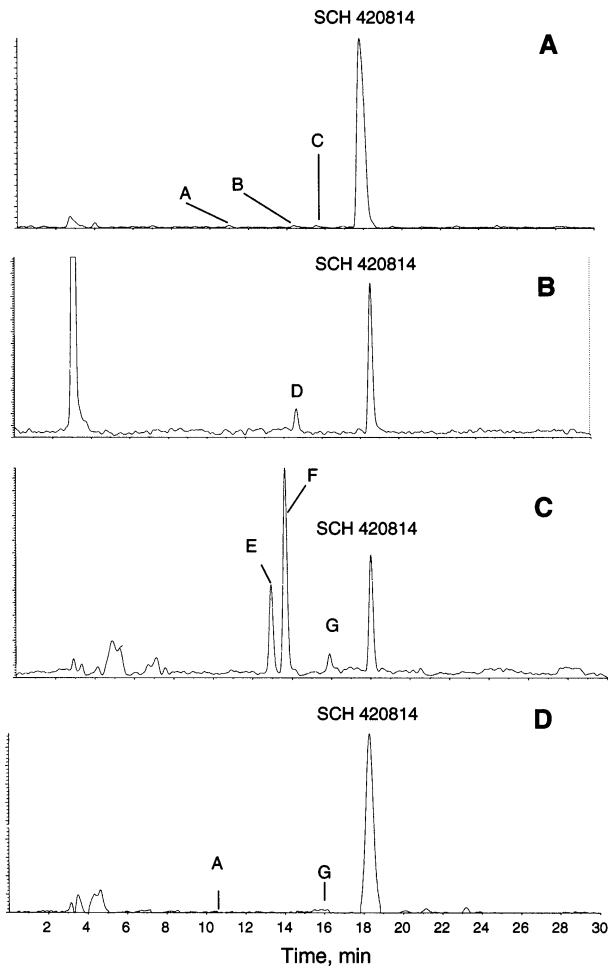

Figure 2. LC-UV chromatograms of the stressed SCH 420814 by 0.1 N HCl for 5 days (A); 0.1 N NaOH for 5 days (B); 1% H_2O_2 for 1 day (C); as well as UV/VIS in a temperature-controlled (25 °C) light chamber (D).

FT MS analysis. The elemental compositions of **A, B** and **C** were established to be $C_{16}H_{20}N_9O$ (MH^+: Cal. 354.1785, found 354.1787; error 0.47 ppm), $C_{24}H_{28}N_9O_3$ (MH^+: Cal. 490.2309, found 490.2312; error 0.48 ppm) and $C_{23}H_{28}N_9O$ (MH^+: Cal. 478.2315, found 478.2318; error 0.60 ppm), respectively.

LC-MS/MS experiments were carried out on the molecular ions of the degradation products in order to obtain their fragmentation patterns for structural analysis. The tandem MS data suggest that compound **A** is a hydrolysis product of SCH 420814 (Scheme 1). Upon CID, the MH^+ ions of compound **A** (*m/z* 354) decompose to give a product-ion spectrum of ions of *m/z* 311, 268, 242 and 113 (Fig. 3(A)). The most abundant fragment ion peak in the spectrum (*m/z* 113) corresponds to a 1-ethylidenepiperazin-1-ium ion (Scheme 1). The product ion at *m/z* 311 is generated by a neutral loss of ethenamine (MW 43) from **A**. The further loss of ethenamine from the ion at *m/z* 311 forms the ion at *m/z* 268 (Scheme 1). Comparing with the formula of SCH 420814 (MH^+: $C_{25}H_{30}N_9O_3$), the component **B** (MH^+: $C_{24}H_{28}N_9O_3$) is a decomposition product via the net loss of a CH_2 group (Scheme 2). Major product ions from the precursor ion (*m/z* 490) were detected at *m/z* 311, 268, 249, 220, 192 and 84 as shown in Fig. 3(B). The most intense peak (*m/z* 249) in the spectrum corresponds to loss of the terminal methyl group from SCH 420814 (Scheme 1). The product ions of *m/z* 220 and 192 originate from *m/z* 249 as proposed in Scheme 1. The structure of degradant **B** was also confirmed with a chemically synthesized standard using LC-UV, LC-MS and LC-MS/MS techniques. The retention time and the product-ion spectrum of the degradation product are identical to those of the standard. Compound **C** is another degradant detected in the acid-stressed SCH 420814. High-resolution FT MS data confirm the difference between the *m/z* 504.2474 (SCH 420814) and *m/z* 478.2318 (compound **C**) is 26.0156 amu or equivalent to a C_2H_2 group. According to the LC/MS/MS data, product ions from the molecular ion (*m/z* 478) were detected at *m/z* 311, 285, 268, 242, 237 and 194, as shown in Fig. 3(C). The abundant fragment ions of *m/z* 311 and 268 are also observed in product-ion spectrum

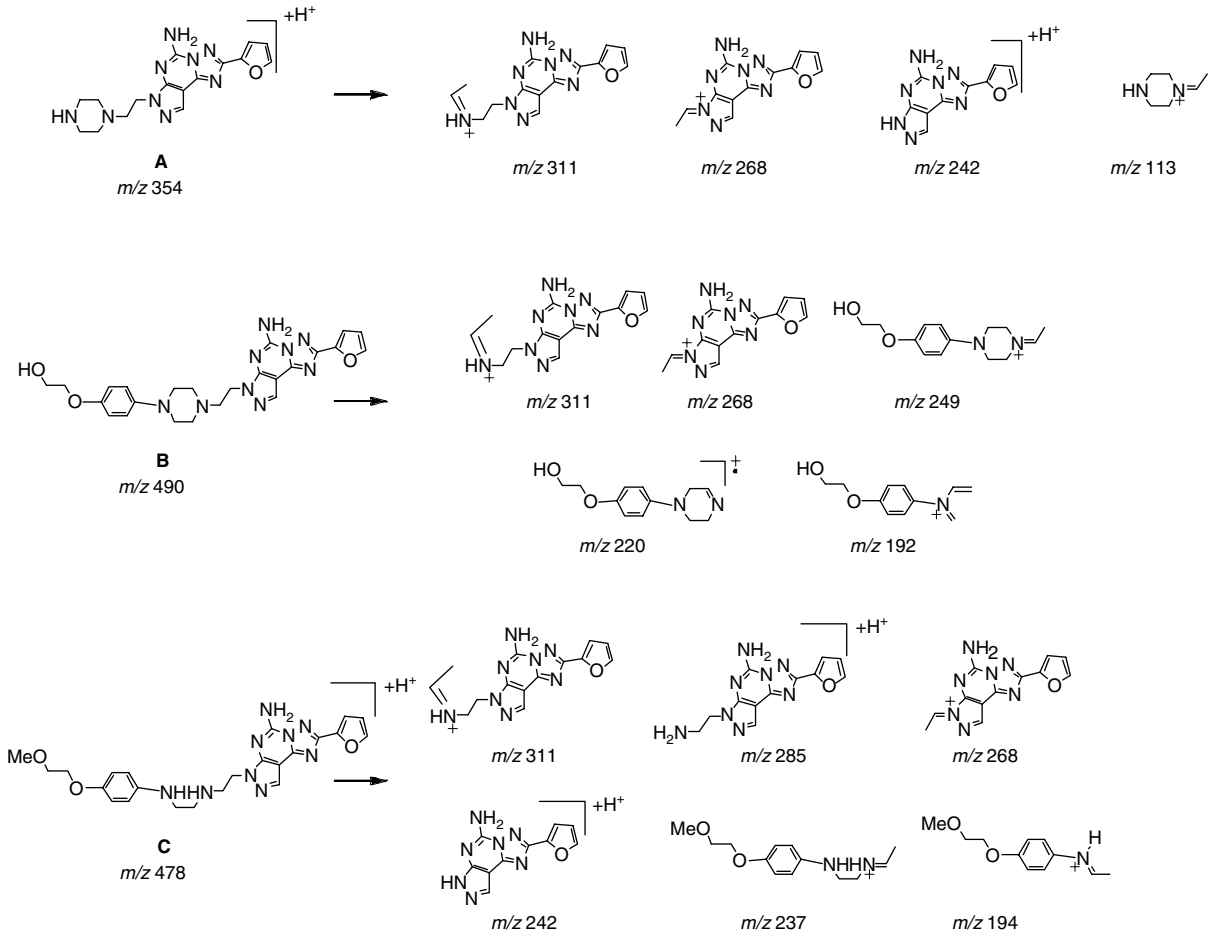

Scheme 1. Proposed fragmentation mechanism for compounds **A, B** and **C**.

of SCH 420814, indicating that the part of the molecule is intact (Scheme 1). The major product ion observed at *m/z* 237 is a crucial evidence for the breakdown of the center piperazine ring, as interpreted in Scheme 1. Moreover, the product ions of *m/z* 285, 242 and 194 are well consistent with the proposed fragmentation mechanism of the compound **C** in Scheme 1.

Studies under basic conditions

There was only one degradation product, **D** (RRT 0.79, *m/z* 522), observed in the LC/MS chromatogram of the basic-stressed sample (Fig. 2(B)). The molecular weight difference of 18 amu between this compound and SCH 420814 (503 Da) suggests that it might be a hydrolysis product of SCH 420814. In order to generate the formula of compound **D**, the basic-stressed sample was submitted to high-resolution FT ESI-MS analysis. However, no ionization was observed for this unknown when it was direct infused into the FT-ICR/MS operating in positive mode. This effect is probably due to the very basic pH of the stressed sample. To overcome the problem, the degradation product was analyzed by LC-FT MS, and the generated data was processed by using DataAnalysis 3.3 software (Bruker). The formula of degradant **D** was confirmed to be $C_{25}H_{32}N_9O_4$ (MH^+: Cal. 522.2571) by applying both internal and external calibrations. The external calibration approach made use of Verapamil and a peptide (ALILTLVS) as calibrants. The internal calibration was performed manually at single point correction mode by using SCH 420814 as calibrant. The accurate mass measurement errors were determined to be −2.2 ppm (MH^+ found: 522.2560) and −3.5 ppm (MH^+ found: 522.2554) for the internal and external calibrations, respectively. A structure was proposed for the compound **D** (Scheme 2) and verified by tandem MS analysis (Fig. 4). Loss of NH_3 from the precursor ion (*m/z* 522) leads to an abundant product ion at *m/z* 505 (Fig. 4, Scheme 2). Further elimination of CO from this ion results a low abundant ion at *m/z* 477 (Scheme 2). The most intense fragment ions of *m/z* 263 and 234 are the same as those observed in the product-ion spectrum of SCH 420814, indicating the hydroxylation does not occur on this part of the molecule (Scheme 2). The product ion of *m/z* 206 originates from *m/z* 263 and 234 as shown in Scheme 2. The product ion of *m/z* 84 is the protonated 1,2,3,6-tetrahydropyrazine. A characteristic product ion of *m/z* 312 fully agrees with the proposed structure of **D** (Scheme 2).

Studies under oxidative conditions

Almost 80% of the drug degraded upon exposure to 1% H_2O_2 for 24 h (Fig. 2(C)). On the basis of the LC/MS(/MS) data of the stressed sample, three unknowns were characterized as compound **E** (RRT 0.71, MW 535), **F** (RRT 0.76, MW 535) and **G** (RRT 0.88, MW 519) (Schemes 3 and 4). According to the LC-UV and LC-MS data, the relative amounts of the degradation products to that of SCH 420814 after the H_2O_2 stress was found to be **F** > **SCH 420814** > **E** > **G**. Comparing with the molecular weight 503 Da of SCH 420814, the unknown **G**, which has an additional 16

Journal of MASS SPECTROMETRY

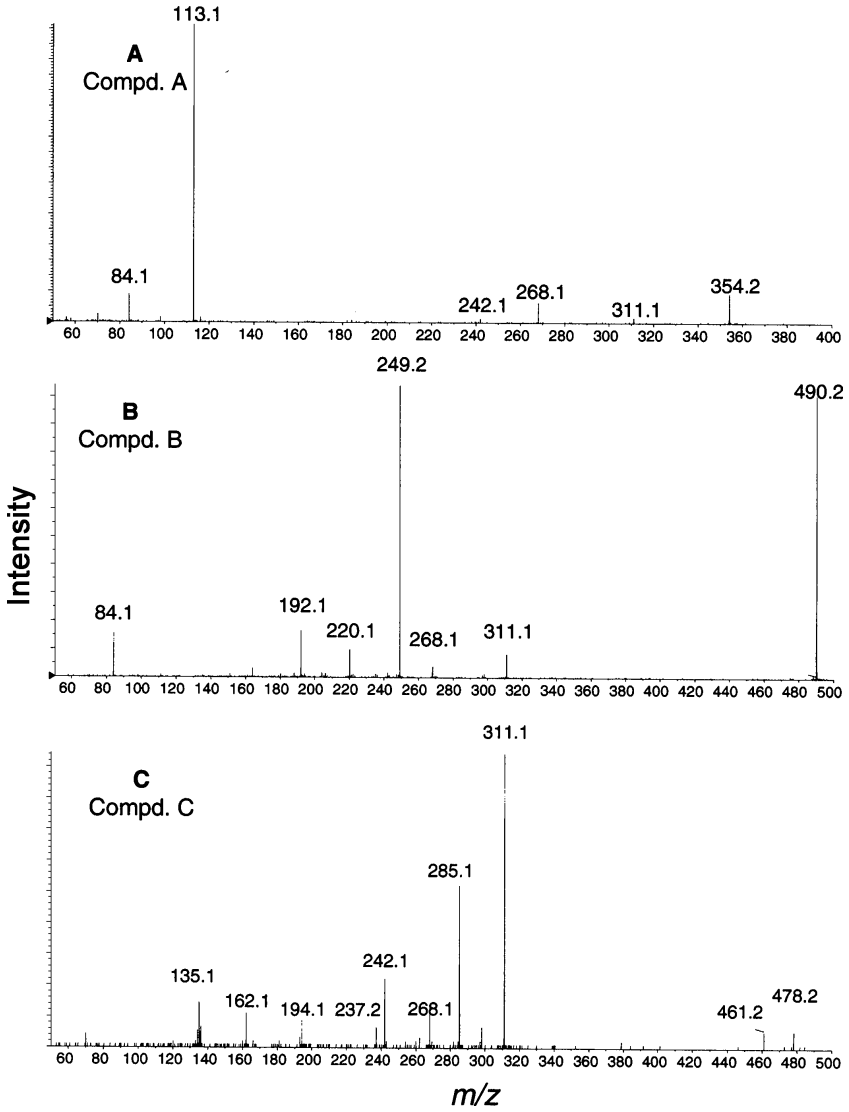

Figure 3. MS/MS product-ion spectra of the protonated molecular ions at *m/z* 354 (A), 490 (B) and 478 (C) for components **A, B** and **C** in Fig. 2A, respectively.

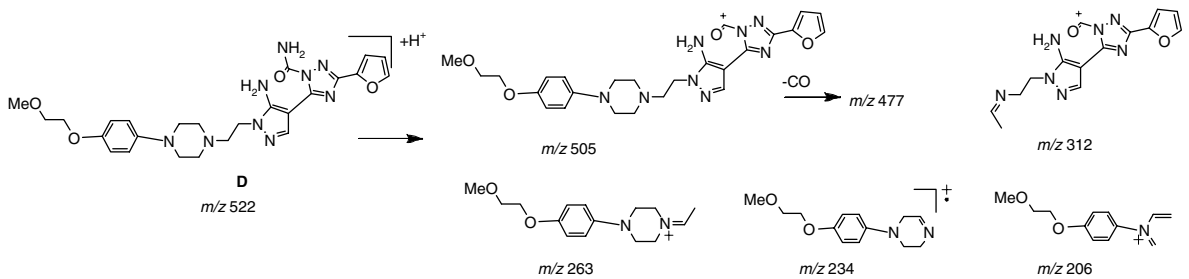

Scheme 2. Proposed fragmentation mechanism for compound **D**.

mass units, may be the oxidized product via the addition of an oxygen atoms. Similarly, unknown **E** and **F** may be the di-oxidation product of SCH 420814. The stressed sample was analyzed by FT MS, and the elemental composition of **E, F** and **G** were confirmed to be $C_{25}H_{30}N_9O_5$ (MH^+: Cal. 536.2364, found 536.2361; error −0.63 ppm), $C_{25}H_{30}N_9O_5$ (MH^+: Cal. 536.2364, found 536.2361; error −0.63 ppm) and $C_{25}H_{30}N_9O_4$ (MH^+: Cal. 520.2415, found 520.2413; error −0.43 ppm), respectively.

The informative tandem MS data reveal the structural information pertaining to the two di-oxidation isomers (Fig. 5). The mass fragmentation pattern for **E** is quite different from that for **F**. Collisional activation of the precursor ion of the **E** results in a number of product ions, with *m/z* 323, 313, 268, 252, 232, 206 and 193, as shown in Fig. 5(A). On the other hand, the collision-induced dissociation of **F** yields major product ions of *m/z* 339, 311, 297, 268, 232 and 194 (Fig. 5(B)). Upon CID, unknown **E** and **F** forms

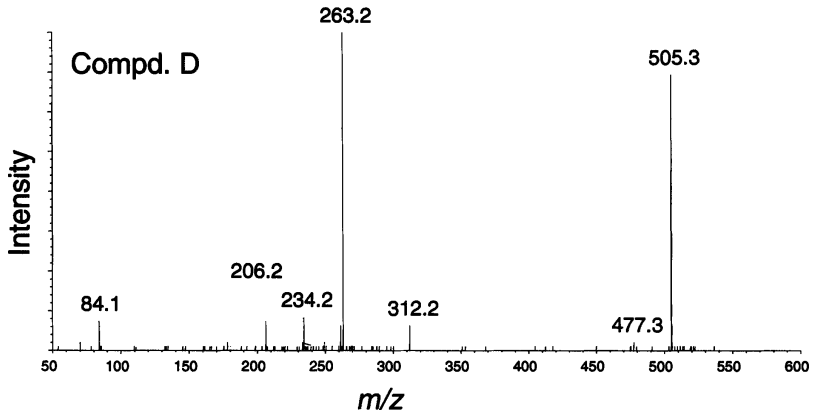

Figure 4. MS/MS product-ion spectrum of compound **D** (*m/z* 505) generated by alkaline stressed conditions.

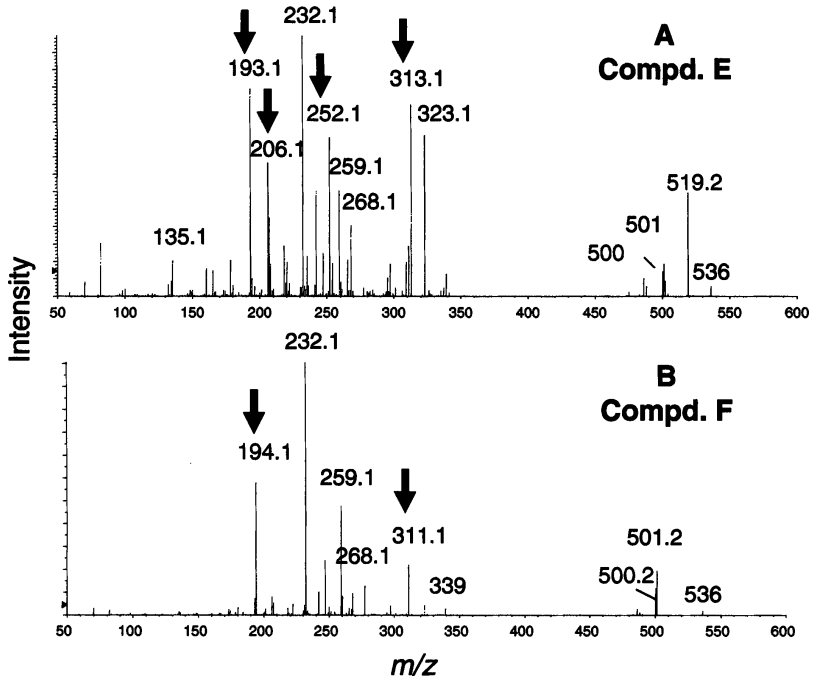

Figure 5. Comparison of the MS/MS spectra of SCH 420814 degradation products **E** (A) and **F** (B) generated by oxidative conditions.

a common fragment ion of *m/z* 268, which was also observed in the product-ion spectrum of SCH 420814. This indicates this part of SCH 420814 is intact (Scheme 3), and the di-oxidation could occur only on the piperazine ring. For both **E** and **F**, the breaking of the carbon-nitrogen bond, followed by consecutive loss of two waters yielded the most abundant ion at *m/z* 232 (Scheme 3). For compound **E**, the piperazine-ring cleavages give rise to two major product ions of *m/z* 313 and 252 (Scheme 3). Further fragmentation of the ion at *m/z* 252 generates product ion at *m/z* 193 via loss of ethene-1,2-diol radical (Scheme 3). Two characteristic product ions of *m/z* 323 and 206 are also consistent with the proposed structure of **E** as shown in Scheme 3. For compound **F**, the through piperazine-ring cleavages leads to product ions of *m/z* 339, 311, 297 and 194 (Fig. 5(B)), and their interpretation are shown in Scheme 3. These distinctive fragment ions of compound **F** are not seen in the product-ion spectrum of **E** (Fig. 5). Thus, the study of the MS/MS fragmentation pathway of the two degradation products allows the rapid and direct differentiation of the two proposed structures (**E** and **F**).

The mono-oxidation product **G** was also identified as a minor degradant of the H_2O_2-stressed SCH 420814 (Fig. 2(C)). The characteristic fragment ions of degradation product **G** are observed at *m/z* 323, 311, 297, 279, 262, 249, 242, 234, 207 and 193 (spectrum not shown), and a fragmentation pathway is proposed in Scheme 4. The product-ion spectrum of **G** clearly indicates the hydroxyl group is locating on the piperazine ring; however, the exact oxidation position cannot be elucidated solely by mass spectrometry (Scheme 4). The most of the fragmentation is occurred at the piperazine components of the molecule (i.e. *m/z* 323, 311, 207 and 193 in Scheme 4). Two complementary fragment ions of the degradation product were detected at *m/z* 279 and 242 (Scheme 4). Recall that the fragment ion of *m/z* 263 is the most abundant one observed in the product-ion spectrum of SCH 420814 (Fig. 1). We believe the ion of *m/z* 279 is formed in an analogous manner and agrees well with our proposed structure of **G** (Scheme 4). The hydroxyl group, however, can locate on either the 2- or 3-position of the piperazine ring (Scheme 4), and the two isomers cannot be easily distinguished by the LC-MS/MS analysis. For further

Journal of MASS SPECTROMETRY

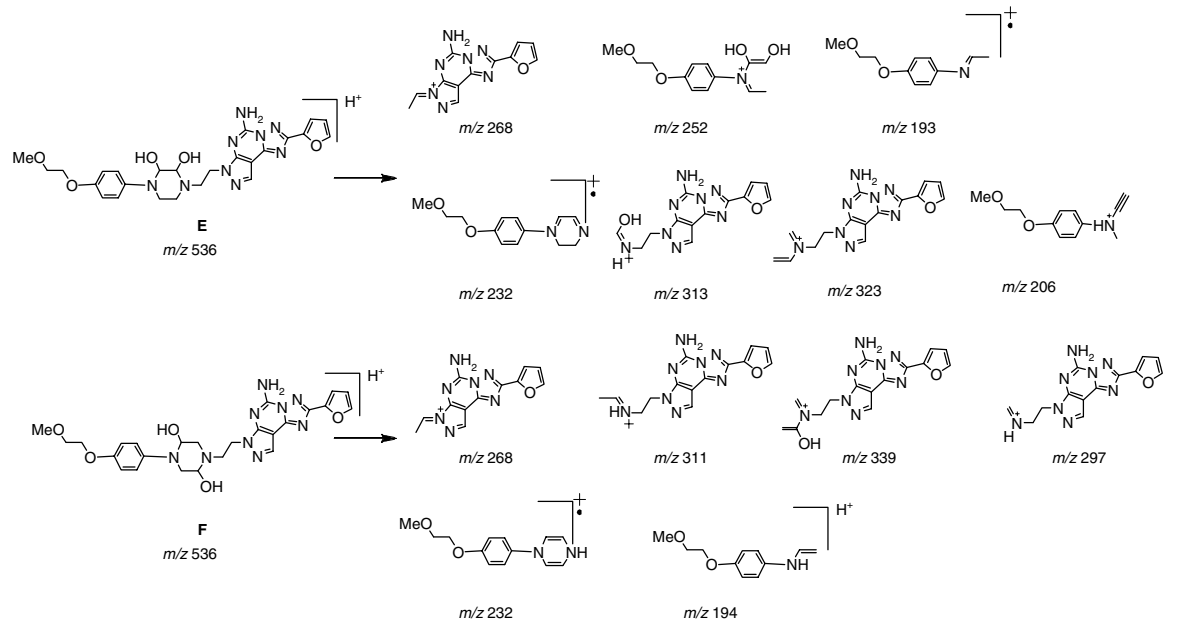

Scheme 3. Proposed fragmentation mechanism for compounds **E** and **F**.

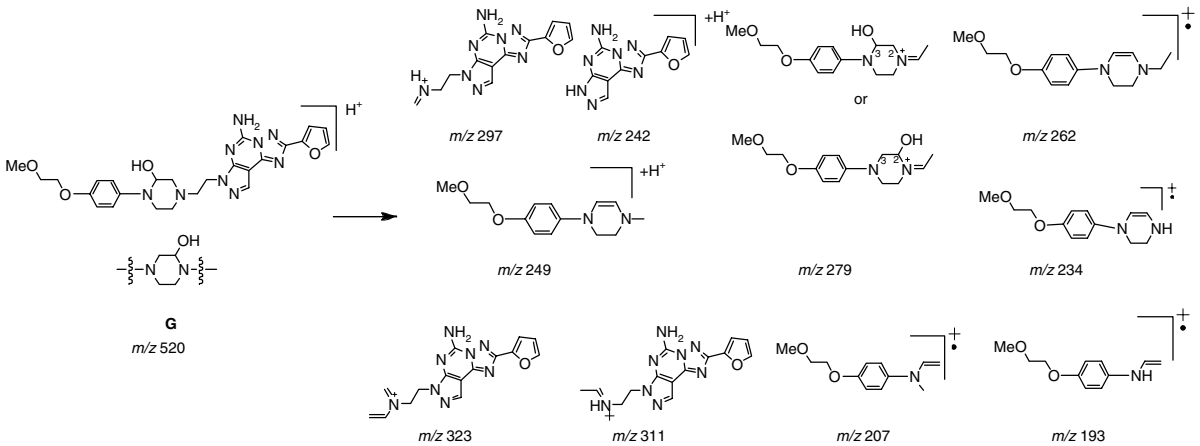

Scheme 4. Proposed fragmentation mechanism for compound **G**.

structural confirmations, the MS and NMR analysis of the synthetic degradation products and/or isolated samples are required.

On the basis of our results, we conclude that the forced oxidations are occurred at the piperazine ring in the center of SCH 420814.

Studies under photolytic conditions

The exposure of SCH 420814 to light (UV/VIS) did not result in any significant degradation (Fig. 2D). Two components eluted at 10.4 and 16.0 min in the LC chromatogram was characterized as **A** (RRT 0.61, MW 353) and **G** (RRT 0.88, MW 520), respectively. The compound **A** had been identified as a degradation product of SCH 420814 under acid stress condition (Scheme 1), whereas the compound **G** is an oxidation product of SCH 420814 (Scheme 4).

Degradation behaviors of the stressed SCH 420814 tablets

The identification of degradant formed in stressed tablets of SCH 420814 (open dish, RH4 for 1 month) was achieved by LC/MS/MS studies. Five major degradation products (**A, C, H, I** and **J**) were detected as shown in Fig. 6. The relative amounts of the degradants to that of SCH 420814 after the RH4 stress was found to be **SCH 420814** $\gg$ **H** $\sim$ **J** $>$ **A** $\sim$ **I** $\sim$ **C** (Fig. 6). The LC-MS analysis confirmed the presence of decomposition products, **A** (RRT 0.61, MW 353) and **C** (RRT 0.87, MW 477), in the stressed sample. These two compounds had been previously identified in the acid-stressed sample. The unknown, **H** (MW 284, RRT 0.56), was determined to be a decomposition product of SCH 420814. The proposed structure (**H**, Fig. 6) was confirmed by tandem MS analysis. The collision-induced dissociation of the *m/z* 285 ion gives product ions of *m/z* 268 ($[MH^+ - NH_3]$, 242, 214, 187, 161 and 134 (product-ion spectrum not shown). The fragmentation pattern of the product-ion spectrum was found to be consistent with the proposed structures (**H**). The most abundant fragment ion (*m/z* 242) was generated by neutral loss of ethenamine from the molecular ion of compound **H**. The other product ions are generated by the fragmentation of the 7H-pyrazolo[4,3-e][1,2,4]triazolo[1,5-c]pyrimidin-5-amine triaromatic ring.

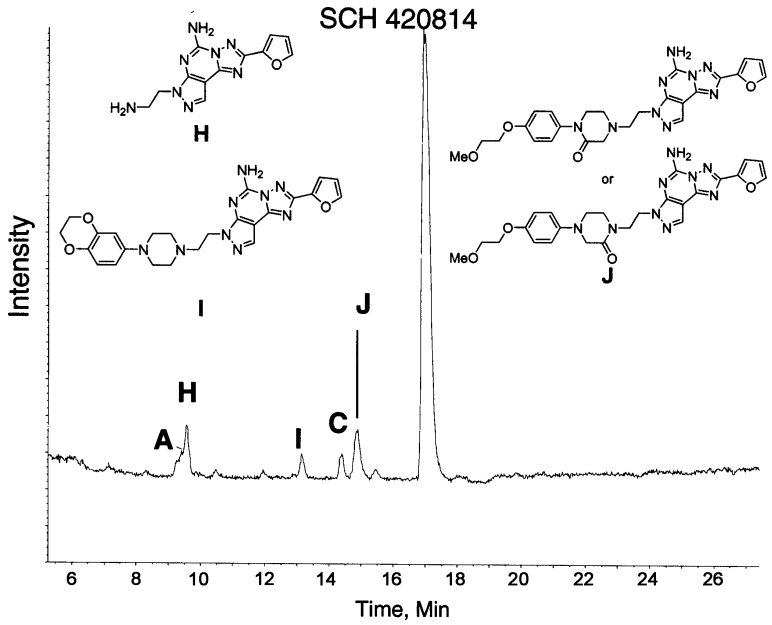

Figure 6. LC-MS chromatogram of the sample extracted from a SCH 420814/excipient capsule which had been stored on an open dish (RH4) for 1 month.

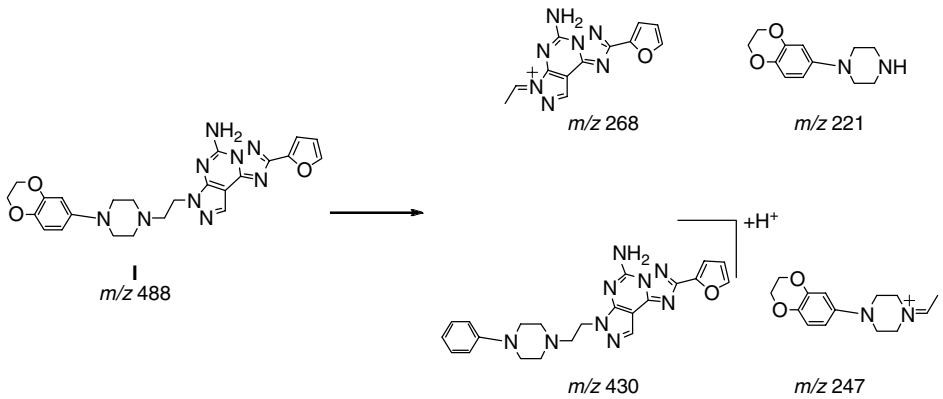

Scheme 5. Proposed fragmentation mechanism for compound **I**.

The LC/MS analysis also confirmed the presence of a unique degradation product, **I** (MW 487, RRT 0.77), in the stressed tablet. The LC-MS/MS product-ion spectrum for product **I** contains a fragment ion of *m/z* 268, indicating this part of SCH 420814 is intact (Fig. 7, Scheme 5). An ion detected at *m/z* 221 is found to be the complementary fragment ion of *m/z* 268 (Scheme 5). In addition, the presence of the fragment ion at *m/z* 430 corresponds to the loss of the diethanol from **I** (Scheme 5). On the basis of the tandem MS data, we proposed structure **I** for this degradation product as shown in Scheme 5. The observation of an abundant fragment ion at *m/z* 247 also agrees well with the structure assignment (Fig. 7, Scheme 5).

A mechanism was proposed for the formation of **I** by heat stress in the solid state (40 °C/75% relative humidity, 1 month) (Scheme 6). In the proposed mechanism, a dienone intermediate (Scheme 6, **I-1**) could be formed directly from SCH 420814. The dienone intermediate (**I-1**) would then undergo an intermolecular ring-closure reaction to form **I-2**, followed by rapid methane loss to yield compound **I** (Scheme 6).

The molecular weight of the unknown **J** (RRT 0.87) was determined to be 517 Da by LC/MS analysis (Fig. 6). The molecular weight of compound **J** is 14 Da higher than that of SCH 420814, which suggests one oxygen atom is added with the removal of two

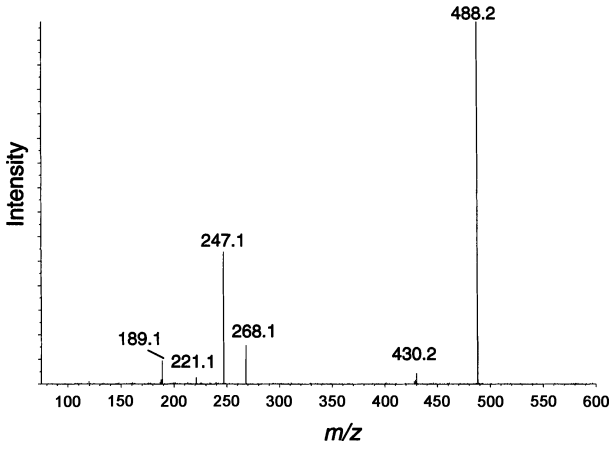

Figure 7. MS/MS product-ion spectrum of the protonated molecular ion at *m/z* 505 for the component **I** in Fig. 6.

Journal of MASS SPECTROMETRY

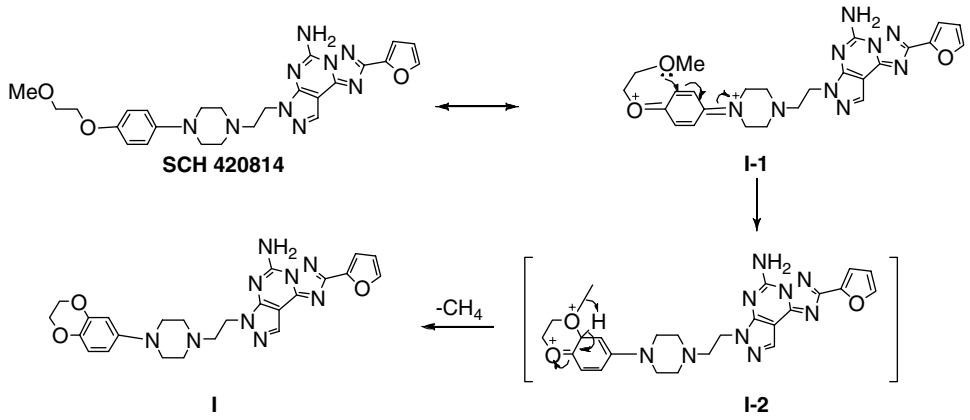

Scheme 6. Proposed mechanism for the formation of **I** by RH4 in the solid state.

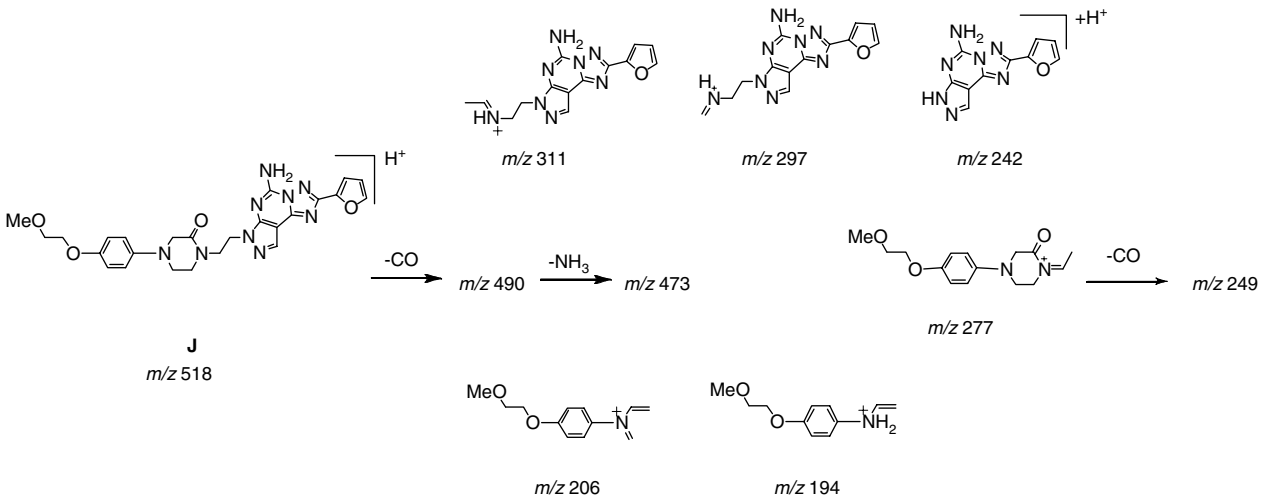

Scheme 7. Proposed fragmentation mechanism for compound **J**.

hydrogen atoms on SCH 420814. The MS/MS product-ion spectrum shows major fragment ions at *m/z* 490, 473, 311, 297, 277, 242, 249, 206 and 194 (spectrum not shown). The consecutive losses of CO and NH_3 from the parent molecular ion (*m/z* 518) yield the product ions at *m/z* 490 and 473, respectively (Scheme 7). The observation of CID product ions at *m/z* 311, 297 and 242 clearly indicates the oxidation of SCH 420814 occurred on the piperazine ring (Scheme 7). The rest of the major fragment ions are also consistent with the proposed structure of the degradation product as shown in Scheme 7.

Conclusions

We demonstrated the application of LC-MS/MS and FT MS for the detection and characterization of the degradation products of SCH 420814. The chromatographic method we described here can resolve all degradation products from the parent as well as from each other. All degradation products were detected, and the relative UV and MS response of the degradation products with respect to the parent was determined. SCH 420814 underwent most degradation under oxidative conditions to yield two major (**E** and **F**) and one minor products (**G**). The degradation was mild under acidic, alkaline and photolytic conditions, forming a total of six products, but in small quantities. The exposure of the drug tablets to RH4 for 1 month resulted in generation of five degradation products also in small quantities.

Acknowledgements

The authors thank Schering-Plough Research Institute for financial support. They also thank Drs Malcolm MacCoss and John Piwinski for their support of this project.

References

[1] B. R. Neustadt, J. Hao, N. Lindo, W. J. Greenlee, A. W. Stamford, D. Tulshian, E. Ongini, J. Hunter, A. Monopoli, R. Bertorelli, C. Foster, L. Arik, J. Lachowicz, K. Ng, K.-I. Feng. Potent, selective, and orally active adenosine A2A receptor antagonists: Arylpiperazine derivatives of pyrazolo[4,3-e]-1,2,4-triazolo[1,5-c]pyrimidines. *Bioorganic & Medicinal Chemistry Letters* **2007**, *17*, 1376.

[2] U. Shah, C. D. Boyle, S. Chackalamannil, B. R. Neustadt, N. Lindo, W. J. Greenlee, C. Foster, L. Arik, Y. Zhai, K. Ng, S. Wang, A. Monopoli, J. E. Lachowicz. Biaryl and heteroaryl derivatives of SCH 58261 as potent and selective adenosine A2A receptor antagonists. *Bioorganic & Medicinal Chemistry Letters* **2008**, *18*, 4199.

[3] U. Shah, C. M. Lankin, C. D. Boyle, S. Chackalamannil, W. J. Greenlee, B. R. Neustadt, M. E. Cohen-Williams, G. A. Higgins, K. Ng, G. B. Varty, H. Zhang, J. E. Lachowicz. Design, synthesis, and evaluation of fused heterocyclic analogs of SCH 58261 as adenosine A2A receptor

antagonists. *Bioorganic & Medicinal Chemistry Letters* **2008**, *18*, 4204.
[4] T. Kenakin. *Understanding G Protein-Coupled Receptors and Their Role in the CNS*. Oxford University Press: Oxford, **2002**.
[5] P. Tuite, J. Riss. Recent developments in the pharmacological treatment of Parkinson's disease. *Expert Opinion on Investigational Drugs* **2003**, *12*, 1335.
[6] C. E. Muller. A2A adenosine receptor antagonists - future drugs for Parkinson's disease?. *Drugs of the Future* **2000**, *25*, 1043.
[7] M. A. Schwarzschild, L. Agnati, K. Fuxe, J.-F. Chen, M. Morelli. Targeting adenosine A2A receptors in Parkinson's disease. *Trends in Neurosciences* **2006**, *29*, 647.
[8] D. H. Slee, X. Zhang, M. Moorjani, E. Lin, M. C. Lanier, Y. Chen, J. K. Rueter, S. M. Lechner, S. Markison, S. Malany, T. Joswig, M. Santos, R. S. Gross, J. P. Williams, J. C. Castro-Palomino, M. I. Crespo, M. Prat, S. Gual, J.-L. Diaz, J. Wen, Z. O'Brien, J. Saunders. Identification of Novel, Water-Soluble, 2-Amino-N-pyrimidin-4-yl Acetamides as A2A Receptor Antagonists with In Vivo Efficacy. *Journal of Medicinal Chemistry* **2008**, *51*, 400.
[9] International Conference on Harmonisation, Stability Testing of New Drug Substances and Products, February 2003.
[10] P. J. Jansen, W. K. Smith, S. W. Baertschi. Stress testing: analytical considerations. *Drugs and the Pharmaceutical Sciences* **2005**, *153*, 141.
[11] K. M. Alsante, L. Martin, S. W. Baertschi. A stress testing benchmarking study. *Pharmaceutical Technology* **2003**, *27*, 60.
[12] J. Wong, L. Wiseman, S. Al-Mamoon, T. Cooper, L. K. Zhang, T. M. Chan. Major Degradation Product Identified in Several Pharmaceutical Formulations against the Common Cold. *Analytical Chemistry* **2006**, *78*, 7891.
[13] F. Erni. Liquid chromatography-mass spectrometry in the pharmaceutical industry: objectives and needs. *Journal of Chromatography* **1982**, *251*, 141.
[14] W. Feng, H. Liu, G. Chen, R. Malchow, F. Bennett, E. Lin, B. Pramanik, T. M. Chan. Structural characterization of the oxidative degradation products of an antifungal agent SCH 56592 by LC-NMR and LC-MS. *Journal of Pharmaceutical and Biomedical Analysis* **2001**, *25*, 545.
[15] M. S. Lee, E. H. Kerns. LC/MS applications in drug development. *Mass Spectrometry Reviews* **1999**, *18*, 187.
[16] B. N. Pramanik, P. L. Bartner, G. Chen. The role of mass spectrometry in the drug discovery process. *Current Opinion in Drug Discovery & Development* **1999**, *2*, 401.
[17] R. A. Rourick, K. J. Volk, S. E. Klohr, T. Spears, E. H. Kerns, M. S. Lee. Predictive strategy for the rapid structure elucidation of drug degradants. *Journal of Pharmaceutical and Biomedical Analysis* **1996**, *14*, 1743.
[18] P. A. Shipkova, L. Heimark, P. L. Bartner, G. Chen, B. N. Pramanik, A. K. Ganguly, R. B. Cody, A. Kusai. High-resolution LC/MS for analysis of minor components in complex mixtures: negative ion ESI for identification of impurities and degradation products of a novel oligosaccharide antibiotic. *Journal of Mass Spectrometry* **2000**, *35*, 1252.
[19] K. J. Volk, S. E. Hill, E. H. Kerns, M. S. Lee. Profiling degradants of paclitaxel using liquid chromatography-mass spectrometry and liquid chromatography-tandem mass spectrometry substructural techniques. *Journal of Chromatography, B: Biomedical Sciences and Applications* **1997**, *696*, 99.
[20] B. E. Winger, C. A. J. Kemp. Characterization of pharmaceutical compounds and related substances by using HPLC FTICR-MS and tandem mass spectrometry. *American Pharmaceutical Review* **2001**, *4*, 55.
[21] Y. Wu. The use of liquid chromatography-mass spectrometry for the identification of drug degradation products in pharmaceutical formulations. *Biomedical Chromatography* **2000**, *14*, 384.
[22] L.-K. Zhang, D. Rempel, N. Pramanik Birendra, L. Gross Michael. Accurate mass measurements by Fourier transform mass spectrometry. *Mass Spectrometry Reviews* **2005**, *24*, 286.
[23] Z. Zhao, Q. Wang, E. W. Tsai, X.-Z. Qin, D. Ip. Identification of losartan degradates in stressed tablets by LC-MS and LC-MS/MS. *Journal of Pharmaceutical and Biomedical Analysis* **1999**, *20*, 129.
[24] T. Murakami, N. Fukutsu, J. Kondo, T. Kawasaki, F. Kusu. Application of liquid chromatography-two-dimensional nuclear magnetic resonance spectroscopy using pre-concentration column trapping and liquid chromatography-mass spectrometry for the identification of degradation products in stressed commercial amlodipine maleate tablets. *Journal of Chromatography, A* **2008**, *1181*, 67.
[25] J. M. Ballard, L. Zhu, E. D. Nelson, R. A. Seburg. Degradation of vitamin D3 in a stressed formulation: The identification of esters of vitamin D3 formed by a transesterification with triglycerides. *Journal of Pharmaceutical and Biomedical Analysis* **2007**, *43*, 142.
[26] D. Breton, D. Buret, A. C. Mendes-Oustric, P. Chaimbault, M. Lafosse, P. Clair. LC-UV and LC-MS evaluation of stress degradation behaviour of avizafone. *Journal of Pharmaceutical and Biomedical Analysis* **2006**, *41*, 1274.
[27] M. Bakshi, S. Singh. ICH guidance in practice: establishment of inherent stability of secnidazole and development of a validated stability-indicating high-performance liquid chromatographic assay method. *Journal of Pharmaceutical and Biomedical Analysis* **2004**, *36*, 769.
[28] M. Bakshi, S. Singh. HPLC and LC-MS studies on stress degradation behavior of tinidazole and development of a validated specific stability-indicating HPLC assay method. *Journal of Pharmaceutical and Biomedical Analysis* **2004**, *34*, 11.
[29] M. Li, B. Chen, M. Lin, A. Rustum. Application of LC-MSn in conjunction with mechanism-based stress studies in the elucidation of drug impurity/degradation product structures and degradation pathways. *American Pharmaceutical Review* **2008**, *11*, 98.
[30] V. V. Mihaleva, O. Vorst, C. Maliepaard, H. A. Verhoeven, R. C. H. de Vos, R. D. Hall, R. C. H. J. van Ham. Accurate mass error correction in liquid chromatography time-of-flight mass spectrometry based metabolomics. *Metabolomics* **2008**, *4*, 171.
[31] T. Bristow, J. Constantine, M. Harrison, F. Cavoit. Performance optimisation of a new-generation orthogonal-acceleration quadrupole-time-of-flight mass spectrometer. *Rapid Communications in Mass Spectrometry* **2008**, *22*, 1213.
[32] A. V. Tolmachev, M. E. Monroe, N. Jaitly, V. A. Petyuk, J. N. Adkins, R. D. Smith. Mass Measurement Accuracy in Analyses of Highly Complex Mixtures Based Upon Multidimensional Recalibration. *Analytical Chemistry* **2006**, *78*, 8374.
[33] H. C. Koefeler, M. L. Gross. Correction of accurate mass measurement for target compound verification by quadrupole time-of-flight mass spectrometry. *Journal of the American Society for Mass Spectrometry* **2005**, *16*, 406.
[34] A. V. Tolmachev, E. W. Robinson, S. Wu, H. Kang, N. M. Lourette, L. Pasa-Tolic, R. D. Smith. Trapped-Ion Cell with Improved DC Potential Harmonicity for FT-ICR MS. *Journal of the American Society for Mass Spectrometry* **2008**, *19*, 586.
[35] D. K. Williams, Jr., D. C. Muddiman. Parts-Per-Billion Mass Measurement Accuracy Achieved through the Combination of Multiple Linear Regression and Automatic Gain Control in a Fourier Transform Ion Cyclotron Resonance Mass Spectrometer. *Analytical Chemistry* **2007**, *79*, 5058.
[36] D. K. Williams, Jr., M. A. Chadwick, T. I. Williams, D. C. Muddiman. Calibration laws based on multiple linear regression applied to matrix-assisted laser desorption/ionization Fourier transform ion cyclotron resonance mass spectrometry. *Journal of Mass Spectrometry* **2008**, *43*, 1659.
[37] E. P. Maziarz, III, G. A. Baker, T. D. Wood. Electrospray ionization Fourier transform mass spectrometry of polycyclic aromatic hydrocarbons using silver(I)-mediated ionization. *Canadian Journal of Chemistry* **2005**, *83*, 1871.
[38] J. M. Herniman, G. J. Langley, T. W. T. Bristow, G. O'Connor. The validation of exact mass measurements for small molecules using FT-ICRMS for improved confidence in the selection of elemental formulas. *Journal of the American Society for Mass Spectrometry* **2005**, *16*, 1100.
[39] X. Feng, M. M. Siegel. FTICR-MS applications for the structure determination of natural products. *Analytical and Bioanalytical Chemistry* **2007**, *389*, 1341.
[40] G. Chen, L.-K. Zhang, B. N. Pramanik. *HPLC for Pharmaceutical Scientists*. Wiley-Interscience: Hoboken, NJ, **2007**.
[41] Y. Bai, D. Galetskiy, E. Damoc, C. Paschen, Z. Liu, M. Griese, S. Liu, M. Przybylski. High resolution mass spectrometric alveolar proteomics: Identification of surfactant protein SP-A and SP-D modifications in proteinosis and cystic fibrosis patients. *Proteomics* **2004**, *4*, 2300.